U.S. Department of Veterans Affairs
Public Access Author manuscript
JCSM Rapid Commun. Author manuscript; available in PMC 2021 April 08.

Published in final edited form as:
JCSM Rapid Commun. 2021 ; 4(1): 24–39. doi:10.1002/rco2.23.

Aging-associated skeletal muscle defects in HER2/Neu transgenic mammary tumor model

Ruizhong Wang[1], **Brijesh Kumar**[1], **Poornima Bhat-Nakshatri**[1], **Mayuri S Prasad**[1], **Max H. Jacobsen**[2], **Gabriela Ovalle**[2], **Calli Maguire**[2], **George Sandusky**[2], **Trupti Trivedi**[3], **Khalid S Mohammad**[3], **Theresa Guise**[3], **Narsimha R Penthala**[4], **Peter A Crooks**[4], **Jianguo Liu**[1], **Teresa Zimmers**[1,6], **Harikrishna Nakshatri**[1,5,6,*]

[1]Department of Surgery, Indiana University School of Medicine, Indianapolis, IN 46202, USA

[2]Department of Pathology and Laboratory Medicine, Indiana University School of Medicine, Indianapolis, IN 46202, USA

[3]Department of Medicine, Indiana University School of Medicine, Indianapolis, IN 46202, USA

[4]Department of Pharmaceutical Sciences, College of Pharmacy, University of Arkansas for Medical Sciences, Little Rock, AR 72205, USA

[5]Department of Biochemistry and Molecular Biology, Indiana University School of Medicine, Indianapolis, IN 46202, USA

[6]Richard L Roudebush VA Medical Center, Indianapolis, IN 46202, USA

Abstract

Background: Loss of skeletal muscle volume and resulting in functional limitations are poor prognostic markers in breast cancer patients. Several molecular defects in skeletal muscle including reduced MyoD levels and increased protein turn over due to enhanced proteosomal activity have been suggested as causes of skeletal muscle loss in cancer patients. However, it is unknown whether molecular defects in skeletal muscle are dependent on tumor etiology.

Methods: We characterized functional and molecular defects of skeletal muscle in MMTV-Neu (Neu+) mice (n= 6–12), an animal model that represents HER2+ human breast cancer, and compared the results with well-characterized luminal B breast cancer model MMTV-PyMT (PyMT+). Functional studies such as grip strength, rotarod performance, and ex vivo muscle contraction were performed to measure the effects of cancer on skeletal muscle. Expression of muscle-enriched genes and microRNAs as well as circulating cytokines/chemokines were measured. Since NF-κB pathway plays a significant role in skeletal muscle defects, the ability of

*Corresponding Author: Harikrishna Nakshatri, BVSc., PhD, C218C, 980 West Walnut St., Indianapolis, IN 46202, USA, 317 278 2238, hnakshat@iupui.edu.

Author Contribution: RW, experimental design and execution, animal breeding, data collection and analyses, and manuscript writing; BK, flow cytometry, PBN, Lab technical support; MSP, Immunofluorescent imaging support; MJ, Histopathology and H&E staining; CM, CD45 image analysis; GO, muscle histopathological data collection; GS, Histopathology and data analysis; TT, KSM and TG, ex-vivo muscle contraction studies; NP, DMAPT synthesis, PAC, DMAPT synthesis; JL, functional limitation studies; TZ, functional limitation studies; HN, study supervision, experimental design, data interpretation and manuscript writing.

Conflict of Interest: PAC and HN are founders of Leuchemix, Inc, which has an interest in developing DMAPT into anti-cancer therapy. However, HN has recently relinquished his interests in Leuchemix. Others have no conflict of interest to declare.

NF-κB inhibitor dimethylaminoparthenolide (DMAPT) to reverse skeletal muscle defects was examined.

Results: Neu+ mice showed skeletal muscle defects similar to accelerated aging. Compared to age and sex-matched wild type mice, Neu+ tumor-bearing mice had lower grip strength (202±6.9 vs. 179±6.8 g grip force, p=0.0069) and impaired rotarod performance (108±12.1 vs. 30±3.9 seconds, P<0.0001), which was consistent with reduced muscle contractibility (p<0.0001). Skeletal muscle of Neu+ mice (n=6) contained lower levels of CD82+ (16.2±2.9 vs 9.0±1.6) and CD54+ (3.8±0.5 vs 2.4±0.4) muscle stem and progenitor cells (p<0.05), suggesting impaired capacity of muscle regeneration, which was accompanied by decreased MyoD, p53 and miR-486 expression in muscles (p<0.05). Unlike PyMT+ mice, which showed skeletal muscle mitochondrial defects including reduced mitochondria levels and Pgc1β, Neu+ mice displayed accelerated aging-associated changes including muscle fiber shrinkage and increased extracellular matrix deposition. Circulating “aging factor” and cachexia and fibromyalgia-associated chemokine Ccl11 was elevated in Neu+ mice (1439.56±514 vs. 1950±345 pg/ml, p<0.05). Treatment of Neu+ mice with DMAPT significantly restored grip strength (205±6 g force), rotarod performance (74±8.5 seconds), reversed molecular alterations associated with skeletal muscle aging, reduced circulating Ccl11 (1083.26 ±478 pg/ml), and improved animal survival.

Conclusions: These results suggest that breast cancer subtype has a specific impact on the type of molecular and structure changes in skeletal muscle, which needs to be taken into consideration while designing therapies to reduce breast cancer-induced skeletal muscle loss and functional limitations.

Keywords

breast cancer; functional limitations; skeletal muscle; cytokines/chemokines; NF-κB

Introduction

Functional limitations impact the ability to remain independent and increase risk of health problems and progression to disability. Cancer-associated functional limitations affect many aspects of life quality, including physical performance, executive function, and emotional health [1, 2]. Cancer survivors within 2 years of cancer diagnosis are significantly more likely to report limitations in their ability to do heavy work, daily routines such as preparing meals compared to healthy reference subjects [2]. It has been reported that breast cancer patients are more likely to have experienced reduced physical function, vitality, and increased bodily pain over time compared to women who remained free of breast cancer [3–5]. Functional limitation is observed in 39% of breast cancer patients and is associated with increased risk of non-cancer cause of death [3]. Functional limitation is found in women <40 age even at the time of breast cancer diagnosis, before drug or surgical intervention [3, 5]. In addition, women with functional limitations are more likely to have one or more comorbid conditions such as arthritis and hypertension compared to those without functional limitations [5]. Furthermore, lower skeletal muscle volume is a poor prognostic factor in breast cancer patients [6]. Unfortunately, underlying mechanism of functional limitations remains unclear, particularly in breast cancer. Thus, there is an unmet need for mechanistic studies and therapeutic interventions for functional limitations in breast cancer.

Breast cancer is a heterogeneous disease with multiple subtypes [7, 8]. Heterogeneous nature of breast cancer is dictated by cell-type-origin of tumors and genomic aberrations, which poses challenges for prevention, treatment, and management of cancer-associated systemic effects [7]. To aid in characterization of molecular subtypes of breast cancers, a series of genetically engineered mouse models have been developed and implemented in preclinical research [9]. For example, MMTV-PyMT (PyMT+) mouse model represents the luminal B intrinsic subtype [9]. Another widely used transgenic mammary tumor model is the MMTV-Neu (Neu+) model and it represents HER2 amplified subtype of breast cancer [10]. Although these models have been used extensively to study cancer progression and metastasis, they are used rarely to study cancer-induced systemic effects, particularly to link molecular phenotypes of tumor with specific systemic defects and therapeutic intervention.

Cytokines and chemokines secreted by tumors have been associated with functional limitations/cachexia as they interfere with host immunity and myogenesis [11, 1213]. Most of these cytokines/chemokines are upstream of and, in some cases, downstream of NF-κB signaling [14]. Thus, muscle loss in cancer patients may be similar to age-associated muscle loss, which is accompanied with systemic inflammation and increased levels of cytokines including Interlukin 1 (IL-1), IL-6, IL-10, IL-13, tumor necrosis factor alpha (TNFα), and granulocyte-macrophage colony-stimulating factor (GM-CSF) [15]. We recently demonstrated that PyMT+ mice develop functional limitations including reduced grip strength and rotarod performance along with dynamic molecular changes in skeletal muscle [16]. These skeletal muscle molecular changes correlated with alterations in circulating cytokines including elevated tumor necrosis factor alpha (Tnfα) and transforming growth factor beta 2 (Tgfβ2). TNFα is an upstream activator of NF-κB signaling pathway [14], while crosstalk between TGFβ and NF-κB signaling through TAK1 and SMAD7 has been reported [17]. NF-κB has dual functions in cancer; it promotes tumor initiation and progression as demonstrated by us and others and regulates skeletal muscle mass by reducing protein synthesis or enhancing degradation of myogenic transcription factors such as MyoD [14, 18, 19]. Muscle-specific transgenic expression of activated IκB kinase beta (IKKβ), which leads to NF-κB activation, causes profound muscle wasting that resembles clinical cachexia [20]. Indeed, we reported that blockade of NF-κB signaling slows tumor initiation and progression, and attenuates tumor-associated functional limitations such as grip strength and rotarod performance in PyMT+ model of breast cancer [16]. These functional restorations were associated with dynamic molecular changes in skeletal muscle. We observed downregulation of Cox IV, a marker of functional mitochondria, in skeletal muscle of PyMT+ mice suggesting dysregulation of energy production by the mitochondria of skeletal muscles. In addition, we observed reduced circulating and skeletal muscle levels of miR-486, a pivotal microRNA associated with proliferation and differentiation of muscle satellite cells to myocytes and skeletal muscle regeneration [21]. Most critically, we reported an intervention strategy where many of the cancer-induced systemic effects could be reversed through pharmacologic inhibition of the NF-κB pathway.

The present study was designed to test whether mammary tumors representing different molecular subtypes of breast cancer produce similar or different systemic effects and response to intervention by the NF-κB inhibitor DMAPT. Neu+ mice displayed several molecular defects in skeletal muscle and circulating cytokines/chemokines profiles that are

distinct from that of PyMT+ mice. For example, while reduced expression of p53, which enhances survival of muscle satellite cells during repair of injured muscle [22], and senescence-associated Hoxa9 [23] in muscle were common in both models, there was minimum overlap in aberration of other signaling molecules. While muscle satellite cell transcription factor Pax7, mitochondrial metabolic regulator Pgc1β and activin receptor type-2B (Acvr2B) were decreased in PyMT+ model [16], none of these molecules was altered in Neu+ model. Neu+ mice showed reduced levels of CD82+ satellite cells as well as CD54+ myogenic progenitors compared to wild type mice [24, 25]. Circulating cytokines also showed model-specific differences; while cachexia-associated Tnfα and Tgfβ2 were elevated in PyMT+ model, Ccl11 was elevated in Neu+ model. As with PyMT+ mice, DMAPT reversed cancer-induced systemic effects in Neu+ mice but the molecular targets of DMAPT were different. Thus, breast cancer subtypes have distinct effects on skeletal muscle and molecular features of tumors need to be taken into consideration while devising strategies to overcome cancer-induced systemic effects.

Materials and Methods

Animals, functional test and drug administration:

Animal protocols were approved by the Institution Animal Care and Use Committee at the Indiana University School of Medicine and were in accordance with guidelines from National Institutes of Health regarding the use and care of experimental animals. Male Neu+ mice on FVB/N background were purchased from Jackson Laboratory and were randomly bred with normal FVB/N females to obtain female heterozygous for Neu oncogenes. Tumor onset and progression were monitored periodically. Body compositions were measured by Echo-MRI (Houston, TX). All functional studies of mice including grip strength and rotarod performance have been described previously [16]. For drug treatment, DMAPT (100 mg/kg, M-F/week) or vehicle (2.5% mannitol) was gavaged starting at 6–8 weeks for PyMT+ mice or at 16–18 weeks for Neu+ mice post birth until the end of the experiment. Age-matched normal female mice were used as controls. Blood and tissues were collected at the time of sacrifice for miRNA, mRNA, and protein preparation or for histological analysis. Time of sacrifice in survival test was based on recommendation of euthanasia by the attending Veterinarian.

Isolation of skeletal muscle stem cells and flow cytometry:

Mammary tumor-bearing PyMT+ and Neu+ female mice, and age-matched non-tumor-bearing control females were sacrificed with CO_2. Approximately 0.5 grams of muscles were dissected from the hind limb of each mouse. Mouse muscle dissociation kit (130–098-305) and mouse satellite cell isolation kit (130–104-268) were used to isolate mouse muscle stem cells (MuSC) following MACS Miltenyi Biotec manufacture's protocols. Purified MuSC were stained with antibodies CD54-APC (116120; Biolegend) and CD82-PE (PA5–13228; Invitrogen) and analyzed as described previously [26]. Stained cells were acquired using a BD LSR II flow cytometer and data were analyzed using FlowJo software. Forward and side scatter were used to ensure that only live cells were considered in the analysis. Gating was done using appropriate PE (555749) and APC (555576) (BD Pharmingen) isotype control antibodies.

Cell culture and conditioned media (CM):

Mouse myoblast C2C12 cells were seeded and maintained in 60 mm plates in DMEM plus 10% FBS. When cells reached 70–80% confluence, media was changed to DMEM containing 2% of horse serum every other day for 5 days to promote differentiation. Mammary tumor cell lines generated from Neu+ and PyMT+ mice were cultured overnight in DMEM plus 10% FBS and changed to serum-free DMEM medium for 24 hours to generate CM. Undifferentiated cells were treated with CMs for 6 hours and harvested for western blotting. Differentiated C2C12 cells were treated with CMs for 6, 12, 24, and 48 hours and harvested for western blotting.

Muscle-specific force measurements:

Intact isolated extensor digitorum longus (EDL) muscles of control and mammary tumor-bearing PyMT+ and Neu+ mice were attached to an isometric force transducer (Aurora Scientific; model 407A) between platinum stimulating electrodes in a glass chamber containing modified Tyrode solution. A force-frequency relationship was determined by measuring muscle contraction force at a range of frequencies (1–200Hz; Aurora Scientific; model 701C) to obtain a maximum tetanic force plateau. An endurance protocol to measure fatigue was run by inducing a tetanic response (70Hz, 300ms) and repeating for 50 cycles (EDL). Stimulation was controlled by Dynamic Muscle Control software and analyzed using Dynamic Muscle Analysis software (Aurora Scientific; DMC v5.300, DMA v5.010). Specific force (kN/m2) was determined by normalizing the absolute force to muscle cross-sectional area with a muscle density constant of 1.056 kg/m2, thus correcting for differences in size.

miRNA and total RNA extraction:

miRNA and total RNA isolation from plasma and skeletal muscle, respectively, have been described previously [16].

Quantitative reverse transcription PCR:

Taqman miRNA Reverse Transcription Kit (Applied Biosystems, #4366597) was used to synthesize cDNAs with 5 microliters of miRNAs extracted from plasma (20 ng/μl). Bio-RAD iScript cDNA synthesis kit (#170–8891) was used to reverse transcribe total RNAs extracted from muscle tissues (200 ng/μl) into cDNAs in a final volume of 20 μL. Quantitative PCR (qPCR) was performed using Taqman universal PCR master mix (Applied Biosystems, #4324018) and specific primers as described in Table S1 and our previous study [16]. miR-202 and U6 small RNA were used as normalization controls for plasma and muscle microRNAs, respectively. Hsp90ab1 was used as a normalization control for all mRNA measurements.

Histological and immunohistochemical (IHC) analyses:

For lung and muscle H&E staining, 10% formalin-fixed tissues were transferred to the pathology lab, paraffin-embedded, sliced, stained, and analyzed by a pathologist blinded to the study. For IHC of skeletal muscles, CD45 (BD-550286) staining was performed at

Indiana University Health IHC core laboratory and analyzed by a pathologist. ECM staining has been described previously [16].

Western blotting:

Harvested cells and mouse muscles (~30 mg tissue) were lysed in RIPA buffer with protease/phosphatase inhibitors (Sigma). Qiagen TissueLyser LT with metal bead was used to homogenize muscles at a speed of 50Hz for 3 min, followed by 10 seconds sonication. Thirty micrograms of proteins were used for Western blotting. Antibody information is included in Table S1. Quantification of western blotting was performed using NIH image J software. Protein levels were normalized to total proteins in lysates by Ponceau S staining [27–29] in case of skeletal muscle lysate or normalized to β-actin of C2C12 cells in culture.

Circulating Cytokines:

Profiling of 32 cytokines/chemokines from limited samples of mouse plasma has been described previously [16]. Tgfβ1, 2, and 3 were measured separately. Each group contained plasma samples from six animals. Those samples with no detectable values were given a score of zero for the analyses.

Statistical analysis.

Data were analyzed using one-way ANOVA with Tukey's multiple comparisons test for comparisons between multiple groups or unpaired parametric t-test for comparison between two groups. A P value of <0.05 was considered statistically significant.

Results

Reduced functional performance of tumor-bearing Neu+ mice

To determine the consequences of tumors on functional limitations, we subjected age-matched control and tumor-bearing Neu+ female mice to functional studies. Tumor-bearing mice displayed reduced grip strength and rotarod performance. At the age of 24 weeks, Neu + tumor-bearing mice had 179±6.8 g grip force, which was significantly lower than 202±6.9 g grip force observed in wild type mice. There was progressive loss of grip strength with tumor growth (Figure S1A). At the age of 28 weeks, Neu+ tumor-bearing mice had 175±8.2 g grip force, while age-matched wild type mice displayed 202±6.1 g grip force (Figure 1A). Rotarod performance of Neu+ mice also differed from the wild type mice. While wild type mice stayed on rods for 108±12.1 seconds, Neu+ mice could stay on rod for only 30±3.9 seconds (Figure 1B). These data suggest that tumor progression in Neu+ mice leads to muscle weakness.

To confirm that the above noted muscle weakness in tumor-bearing mice is due to defect in skeletal muscle function and is not an indirect consequence of tumor burden hampering movement, we measured muscle specific force using isolated extensor digitorum longus (EDL) muscle. A force-frequency relationship was determined by measuring contraction force at range of frequencies to obtain a maximum tetanic force plateau. Muscle contraction force frequency was significantly lower in EDL of Neu+ mice compared to age matched control mice (Figure 1C). Similar results were obtained with EDLs of PyMT+ mice (Figure

1D). Thus, cancer-mediated reduction in grip strength and rotarod performance correlates with reduction in muscle contraction force.

To determine whether NF-κB signaling pathways are involved in reduction of functional performance and inhibitors of this pathway could improve muscle function in tumor-bearing Neu+ mice, we orally administrated NF-κB inhibitor DMAPT starting at the age of 16 weeks, prior to visible appearance of tumors, till the end of the experiment [16]. DMAPT prevented the cancer-induced reduction of grip force, as there was no significant difference in grip forces between DMAPT treated group and wild type group during observation period (Figure 1A; Figure S1B). Also note that even when tumor volume was similar between vehicle-treated and DMAPT-treated groups, although at different age, animals in DMAPT-treated group compared to vehicle-treated group displayed higher grip strength (Figure S1). Similar effects of DMAPT were observed in the rotarod performance study. DMAPT-treated Neu+ mice stayed on rod for 74±8.5 seconds, which was much longer than time stayed by the vehicle-treated Neu+ mice (Figure 1B). With respect to other body composition changes, DMAPT improved body lean mass in tumor-bearing mice although tumor itself had minimum effect on lean body mass (Figure S2). Three week treatment with DMAPT did not affect the grip strength and rotarod performance in wild type mice (Figure S3). These results indicate that NF-κB signaling pathway plays a role in reducing muscle function in Neu+ mice, similar to PyMT+ mice [16], and NF-κB inhibitors are potential therapeutic agents to improve quality of life. However, NF-κB inhibition in the absence of tumor-induced hyperactivation is not associated with improved skeletal muscle function.

The skeletal muscle of Neu+ mice contains lower levels of a subgroup of satellite cells that contribute to muscle regeneration

Skeletal muscle satellite cells play an indispensable role in muscle homeostasis and in muscle repairs after injury [30]. Satellite cells correspond to a heterogeneous population of cells and a recent study showed that CD82 is a prospective marker for isolation of human muscle long-term repopulating satellite cells [24]. CD82+ cells are lower in the skeletal muscle of patients with muscular dystrophy and isolated human CD82+ muscle cells readily engraft into muscle in immune-deficient mouse model of muscular dystrophy [24]. CD82 is functionally involved in muscle function as shRNA knockdown of CD82 reduced myoblast proliferation. CD54 is a cell surface marker on Pax7-induced myogenic progenitors that contribute to long-term muscle regeneration *in vivo* [25]. CD82 is expressed constitutively in mouse myoblast cell line C2C12, whereas CD54 in mouse muscle is expressed upon conditioning or upon damage and regeneration in case of Mdx mice [31, 32]. To understand whether mammary tumor-induced functional limitation is associated with altered muscle stem-progenitor-mature cell hierarchy, we isolated skeletal muscle satellite cells from Neu+ and PyMT+ mice, and analyzed MuSC population by flow cytometry using antibodies against cell surface CD82 and CD54. We found that the percentage of CD82+ cells was significantly lower in mammary tumor-bearing Neu+ mice compared to non-tumor-bearing wild type mice (Figure 2A; top panel). Decline in CD54+ muscle progenitor cells was also observed only in case of Neu+ mice. By contrast, CD82+ cells were higher with no change in CD54+ cells in the skeletal muscle of PyMT+ mice (Figure 2B, bottom panel). Note that Neu+ and PyMT+ mice were of different ages at the time of skeletal muscle analyses.

Overall, these results suggest that stem/progenitor hierarchy of skeletal muscle is impaired in Neu+ mice.

The effect of tumors on skeletal muscle gene expression.

The above observation of different skeletal muscle cell composition in Neu+ and PyMT+ mice compared to control mice prompted us to determine gene expression changes in the skeletal muscle of Neu+ mice. We analyzed the expression of genes that have previously been shown to be associated with myogenesis and are part of the commercial myogenesis array [16]. Among 12 genes examined, Hoxa9, Dmpk and Prkag1 mRNA levels were significantly lower in Neu+ mice compared to wild type mice (Figure 3A). DMAPT restored mRNA levels of Hoxa9 and Dmpk, but not mRNA level of Prkag1. Pax7 and Pgc1β, which were lower in the skeletal muscle of PyMT+ mice [16], were unaffected in Neu+ mice. Interestingly, treatment with DMAPT increased mRNA levels of Pgc1β, Pax7, MyoD, Acvr2b, Casz1, Kmt2, Nurr1 and Myf6 in the skeletal muscle of Neu+ mice compared to wild type mice (Figure 3A) suggesting that reducing NF-κB activity can boost the expression levels of several functionally important genes in the skeletal muscle. We verified DMAPT-mediated increase in MyoD by western blotting (Figure 3B and C). Note that cancer-induced decline in Hoxa9 mRNA and DMAPT-mediated increase in MyoD protein in the skeletal muscle are the shared features of Neu+ and PyMT+ mice [16].

A recent study demonstrated an important role for p53 in preventing mitotic catastrophe of aged MuSC and thus enhancing muscle regeneration upon injury [22]. Notch signaling pathways in muscle niche maintain p53 levels by reducing the levels of its inhibitor Mdm2 through the transcription repressor Hey 1 [22]. Since few of the changes in the skeletal muscle of Neu+ mice showed similarities to accelerated aging process, we examined the levels of p53 in skeletal muscle of control and tumor-bearing mice. Indeed, protein levels were lower in the skeletal muscle of Neu+ mice compared to control mice (Figure 3B and C). Interestingly, total p53 mRNA was also lower, but we did not find any differences in Mdm2 levels between three groups, despite reduced Hey 1 mRNA in the skeletal muscle of tumor-bearing mice compared to control mice (Figure 3D). Thus, decline in p53 in the skeletal muscle of Neu+ mice is independent of Notch-Hey 1-Mdm2 axis (Figure 3D). However, DMAPT treatment restored p53 levels suggesting the involvement of NF-κB in repressing p53, which is consistent with the previous report of direct repression of p53 by NF-κB [33].

Since, to our knowledge, this is the first study to find lower p53 levels in skeletal muscle of tumor-bearing mice compared to control mice, we extended the study to PyMT+ model to determine whether tumor-induced loss of p53 in the skeletal muscle is more common. Indeed, p53 levels were lower in the skeletal muscle of PyMT+ mice compared to age matched controls (Figure 3E). DMAPT treatment restored the levels of p53 suggesting the involvement of NF-κB pathway in reducing p53 in the skeletal muscle in this model also. Thus, reduction in p53 activity in the skeletal muscle is common in the both breast cancer models.

To further confirm loss of p53 in the skeletal muscle of tumor-bearing mice, we isolated and purified skeletal muscle cells from control and tumor-bearing mice and examined p53 protein by western blotting. Similar to above results, p53 protein levels were significantly

lower (~80%) in the skeletal muscle cells of tumor-bearing mice compared to control mice (Figure 3F and Figure S4A).

We used C2C12 myoblast cell line model to determine whether loss of p53 occurs in undifferentiated or differentiated muscle cells upon exposure to soluble factors from cancer cells. Undifferentiated and differentiated C2C12 cells were treated with CM from PyMT+ and Neu+ mammary tumor-derived cell lines and p53 levels were measured. While the tumor cell line-derived CM had no effect on p53 levels in undifferentiated cells, CM from Neu+ mice profoundly reduced the levels of p53 in differentiated cells after 6 hours treatment (Figure 3G). The reduction was approximately 50% (Figure S4B). Reduction in p53 levels in differentiated C2C12 cells was observed even after 48 hours of CM treatment (Figure S4C).

DMAPT is effective in restoring circulating and skeletal muscle miR-486 in Neu+ mice.

We had previously reported that despite improving skeletal muscle function, DMAPT failed to restore miR-486 levels in the PyMT+ model [16]. PyMT+ model is an acute model where animals could be treated for only 10 weeks (from 6-weeks age to 15-weeks age), whereas Neu+ model is a chronic model where animals are treated for 17 weeks (from 16-weeks age to 32-weeks age). Unlike in the PyMT+ model, treatment with DMAPT completely restored circulating miR-486 level, and partially restored miR-486 level in the skeletal muscles of mammary tumor-bearing Neu+ mice (Figure 4).

With respect to skeletal muscle expression of other myogenic microRNAs, two models differed significantly. Compared to skeletal muscle of the PyMT+ mice, which contained lower levels of miR-16, miR-146a, miR-214, and miR-206 [16], Neu+ mice skeletal muscle showed minimal changes in these microRNAs compared to control mice (Figure 4 and Table 1).

Neu+ mice contain elevated levels of circulating “aging factor” Ccl11.

In our previous study, we demonstrated that tumor cells themselves secrete several cytokines/chemokines and the tumor genome has an influence on the types of cytokines/chemokines secreted by cancer cells [34]. For example, while tumor cell lines derived from both PyMT+ and Neu+ mice secreted Tnfα, Ccl2, Gm-Csf, Ifnγ, and Il-1α, only Neu+ mice tumor derived cell line secreted G-Csf, Ccl1, Ccl5, Cxcl1, Cxcl2, Cxcl10 and Il1ra. Timp1 was unique to the PyMT+ mice tumor derived cell line. To determine whether these differences in cytokine/chemokine profiles between two models are evident among circulating cytokines/chemokines, we measured cytokine/chemokines in the sera of Neu+ mice and compared their levels with circulating cytokine/chemokine levels in PyMT+ mice described in our previous study [16] (Figure 5 and Table S2). While upregulation of Tgfβ2 was unique to PyMT+ mice, upregulation of Ccl11 (also called eotaxin-1) was unique to Neu+ mice. Interestingly, a recent study showed specific upregulation of Ccl11 in HER2+ breast tumors [35]. Ccl11 has recently been described as an aging factor [36]. We also observed reduced levels of circulating Il-17 in only Neu+ mice compared to control mice, suggesting that the immune response/environment are different in two models.

To determine DMAPT treatment mediated restoration of skeletal muscle function correlates with reversal of tumor-induced changes in cytokine/chemokine profiles or general decline in pro-inflammatory cytokines/chemokines, we compared cytokine/chemokine profiles between vehicle-treated and DMAPT-treated tumor-bearing mice. Treatment with DMAPT resulted in generic decline in pro-inflammatory cytokines/chemokines rather than changes in cancer-specific cytokines/chemokines. For example, DMAPT-treatment resulted in lower levels of circulating Tnfα, Il-1α, Il-2, Il-7, Il-10, Il-12, Il-15, Mcp-1, M-csf, Tgfβ1, Tgfβ2, and Mip2 in Neu+ mice compared to vehicle treated mice, although levels none of these cytokines/chemokines was significantly elevated in tumor-bearing mice compared to wild type mice (Figure 5). Cytokines such as Tnfα, Il-1α, and Mcp-1 are transcriptional targets of NF-κB [37]. Among tumor-specific cytokines/chemokines, DMAPT restored the levels of Il-17 and lowered tumor-induced Ccl11. Therefore, tumor genome has an influence on circulating cytokines/chemokines, which has distinct effects on the skeletal muscle.

Neu+ tumor-induced dynamic changes in skeletal muscle structures.

Since Neu+ mice contained elevated levels of circulating aging factor Ccl11, we determined whether the skeletal muscles of Neu+ muscle show aging-associated changes including muscle fiber size. Indeed, H&E staining of cross-sliced quadriceps revealed remarkable focal shrinkage of skeletal muscle fibers (Figure 6A, arrow, top row), similar to focal shrinkage observed in aging muscle [22]. Image analysis showed that approximately 55±3.6% total cross area of quadriceps was occupied by shrunk muscle fibers in Neu+ mice, which was significantly higher compared to approximately 34±2.6% in wild type mice. Treatment with DMAPT reduced the area occupied by shrunk muscle fibers to approximately 31±7.1%, which was close to the levels in wild type mice. However, mammary tumors in PyMT+ mice did not affect the size of skeletal muscle fibers and treatment with DMAPT did not change the size of skeletal muscle fibers [16].

Our previous study showed downregulation of Pgc1β with accompanying decline in mitochondria numbers, as measured by Cox IV staining, in PyMT+ mice [16]. We examined whether similar changes occur in Neu+ mice. Neither Pgc1β nor mitochondria levels were altered in Neu+ mice compared to control mice (Figure 6B; middle row). Thus, the skeletal muscle mitochondrial defects are unique to PyMT+ mice.

Advancing age is associated with accumulation of extracellular matrix (ECM) proteins in the skeletal muscle [38] and we had previously reported excessive ECM deposition in the skeletal muscle of PyMT+ compared to wild type mice [16]. Interestingly, similar increase in ECM deposition in the skeletal muscle was observed in Neu+ mice (Figure 6C; bottom row). In wild type mice, ECM occupied 11.3±0.6% of area of cross-sectioned muscle, while it was 21.7±1.1% in Neu+ mice. As with PyMT+ mice, treatment with DMAPT attenuated mammary tumor-associated ECM deposition, as ECM levels came down to 13.2±0.6% of area of cross-sectioned muscle. Thus, in both models, a NF-κB-dependent signaling pathway is responsible for elevated ECM deposition, which can be reversed pharmacologically. Collectively, these results imply that certain but not all structural changes in skeletal muscle are tumor subtype-specific.

As a last measure of pro-inflammatory phenotype in the skeletal muscle of tumor-bearing mice, we determined the levels of CD45 in skeletal muscle. CD45 is a receptor-linked protein tyrosine phosphatase that is expressed on all leucocytes and plays a crucial role in cancer-associated inflammation [39]. Our expectation was that the skeletal muscle of tumor-bearing mice would have higher number of CD45+ leucocytes compared to control mice if there is persistent inflammatory phenotype in muscle. Indeed, IHC revealed a trend of elevated CD45 cells in the skeletal muscles of Neu+ mice with vehicle or with DMAPT treatment, when all positive CD45+ cells (weak positive, positive and strong positive CD45+ cells) were included per analysis by the pathologist (Figure S5). Interestingly, when only positive and strongly positive CD45+ cells were counted, there were approximately 5108 CD45+ cells per mm^2 of skeletal muscle of Neu+ mice, while it was significantly lower in wild type mice (419 cells per mm^2) (Figure S5). Treatment with DMAPT did not modify tumor-induced enhancement of leucocyte filtrations, as skeletal muscle of DMAPT-treated mice contained 5932 cells per mm^2. These results suggest that DMAPT modulates muscle function downstream of leukocyte infiltration.

DMAPT slows tumor growth and improves survival of Neu+ mice.

Although mammary tumor development in Neu+ mice is relatively slow compared to PyMT + mice [10, 40, 41] and visible tumors appeared at the ~16–20 weeks post birth date, the numbers and volume of mammary tumors increased with the disease progression (Table S3) and are comparable to mammary tumors in PyMT+ mice at younger age. For example, the average volume of mammary tumors was 0.2±0.10 cm^3, 3.6±1.2 cm^3, and 10.6±1.6 cm^3 at age of 10 weeks, 12 weeks and 14 weeks, respectively, in PyMT+ mice [16], while the average volume of mammary tumors was 0.15±0.08 cm^3, 3.1±1.08 cm^3, and 7.05±1.98 cm^3 at age of 24 weeks, 26 weeks and 28 weeks, respectively, in Neu+ mice (Table S3). In response to treatment with DMAPT starting at 16 weeks of age, tumor onset was delayed, tumor growth rate was reduced (Table S3) and, as a consequence, treated animals survived for a prolonged period compared to vehicle treated mice (Figure S6). Thus, DMAPT not only improved skeletal muscle function but also improved overall survival. These effects of DMAPT is less likely due to the effects of drugs on metastasis as, unlike in PyMT+, Neu+ mice showed very little metastasis to lungs (data not shown). In addition, none of these effects of DMAPT is cardiac-related, as Neu+ mice showed minimum cardiac defects compared to control mice (Figure S6).

Discussion

Functional limitation is mechanistically concomitant with paracrine effects of cancer and is likely due to aberrant myogenesis program and skeletal muscle repair leading to skeletal muscle dysfunction. Lack of clinical success with therapies to overcome functional limitation suggests the need for a radically different approach to treat systemic effects of cancer [42]. Here, we took advantage of well-established animal models of breast cancer, PyMT+ and Neu+ tumor models, to examine whether the tumor subtypes with distinct genomic aberrations show skeletal muscle defects that are molecularly different. Indeed, we observed distinct molecular changes in the skeletal muscles of PyMT+ and Neu+ mice, representing luminal B and Her2+ subtypes of breast cancer, respectively [9]. While reduced

expression of MuSC transcription factor Pax7 and mitochondrial dysfunction were observed only in PyMT+ model [16], significantly reduced size of skeletal muscle fibers, reminiscent of accelerated aging and human muscular dystrophy [43, 44], was observed in Neu+ mice. In addition, both models differed in circulating microRNAs and cytokines/chemokines profiles. These results indicate that cancer-specific genomic aberrations have a critical impact on the type of molecular changes in the skeletal muscle.

Aging-associated changes in the skeletal muscle of mammary tumor-bearing Neu+ mice:

Several changes in the skeletal muscle of Neu+ mice are reminiscent of accelerated aging process. For example, aging is associated with loss of skeletal MuSC function and muscle fiber shrinkage [44, 45], which were observed in the skeletal muscle of Neu+ mice. Aging-associated changes in circulating miR-486 levels are also reported [46]. miR-486, which is enriched in the skeletal muscle and accounts for 21% of total miRNA sequence reads in the skeletal muscle, is an integral part of a myogenesis signaling network that involves Pax7, MyoD, myostatin, and NF-κB [47, 48] and aging-associated inflammatory changes likely disrupts this axis. Systemic inflammation due to Neu+ tumors may have accelerated skeletal muscle aging process. In this regard, Ccl11 has recently been shown to reduce self-renewal of MuSC, although the study was done with MuSC that gave rise to rhabdomyosarcoma [49]. It is interesting the Ccl11 has recently been described as an “aging factor” and is linked to aging-associated decline in adult neurogenesis, and impaired learning and memory [36]. It remains to be determined whether circulating Ccl11, enriched in Neu+ mice, is responsible for aging-associated skeletal muscle defects in Neu+ mice.

Circulating cytokines/chemokines and tumor latency may determine the type of molecular changes in skeletal muscle:

Cytokines/chemokines responsible for muscle dysfunction are the potential targets for therapeutic intervention to improve quality of life. However, this therapeutic approach may need to be individualized, as we noticed model-specific variations in circulating cytokines/chemokines. While Tgfβ2 and Tnfα are the major cytokines implicated in PyMT+ mice [16], Ccl11 is the major chemokine elevated in Neu+ mice. Our observations may be relevant in clinic as another recent study demonstrated molecular subtype specific variations in CC family chemokines within breast tumor tissues and observed specific upregulation of Ccl11 transcripts in HER2+ breast cancers [35]. In addition of aging-associated increase, elevated Ccl11 is observed in patients with fibromyalgia [50] and fibromyalgia is more common in breast cancer patients compared to general population [51]. Patients with fibromyalgia demonstrate structural defect including small fibers in skeletal muscle [52]. Thus, at least in case of HER2+ breast cancers, elevated Ccl11 could promote fibromyalgia and consequently affect skeletal muscle function. Ccl11 could directly affect signaling in skeletal muscle as skeletal muscle expresses its receptor Ccr3 as per GTEx database [53]. Mechanisms involved in Ccl11 upregulation in cancer remains to be explored although the involvement of NF-κB pathway cannot be ruled out as IKKβ, an inducer of NF-κB, is required for Ccl11 expression in intestinal epithelial cells [54] and DMAPT reduced Ccl11 levels in Neu+ mice (Figure 5). Additional studies are needed to determine whether therapies that limit Ccl11 function reduce cancer-induced functional limitations and improve quality of life and survival.

Muscle regeneration-associated Hoxa9 and p53 are impaired in both models:

Our two models appear to recapitulate phenotypes often observed in other skeletal muscle-associated diseases [55], as we observed reduced expression of MuSC-enriched transcription factor Hoxa9 in skeletal muscle of tumor-bearing mice compared to control mice. Activation of Hoxa9 is observed in MuSCs of aged but not young mice upon injury and the activated Hoxa9 impairs recovery and depletion of Hoxa9 restores satellite function in aged muscle [23]. Paradoxically, we observed loss of Hoxa9 expression in skeletal muscle in both of our tumor models suggesting unique regulation of Hoxa9 in skeletal muscle of cancer-bearing mice or Hoxa9 loss is a reaction of skeletal muscle to overcome the deleterious effects of tumors on satellite cell function.

Reduced skeletal muscle level of p53 was found in both models suggesting cancer-induced defect in skeletal muscle regeneration. In aged mice, p53 deficiency leads to impaired self-renewal and increased mitotic catastrophe of MuSC during repair process [22]. Reduced skeletal muscle p53 levels may also be responsible for lower expression of miR-486 in skeletal muscle as well as lower circulating levels, as a recent report indicated p53-mediated positive transcriptional regulation of miR-486 [56, 57]. In our present study, DMAPT treatment reversed the loss of p53 in skeletal muscles of Neu+ mice, which is consistent with restoration of miR-486 in circulating system and skeletal muscles in DMAPT-treated mice (Figure 4). In addition to miR-486, p53 loss could impact other pathways of myogenesis as p53 controls expression/activity of Carm1, a major epigenetic regulator of MuSC asymmetric division, and Prdm16, which controls MuSC differentiation into brown adipose tissue [30, 58, 59].

How tumor burden leads to lower skeletal muscle p53 is unclear at present. The previously described Notch-Hey1-Mdm2 axis [22] is less likely involved, as we did not observe differences in skeletal muscle Mdm2 levels in control and tumor-bearing mice. Based on the literature [33] as well as the ability of NF-κB inhibitor DMAPT to reverse p53 loss, cancer-mediated induction of NF-κB in skeletal muscle could be responsible for reduced p53 levels. Collectively, these results reveal a NF-κB:p53:miR-486 axis involved in myogenic signaling network and the role of tumors in disrupting this axis to cause skeletal muscle disfunction.

Types of molecular changes in skeletal muscle may depend on tumor latency.

The aggressive PyMT+ model (~105 days), which has tumor gene expression pattern resembling luminal B breast cancer [9], displayed many more musculoskeletal defects compared to less aggressive Neu+ model (~220 days). MuSC exhaustion appears to be much more extreme in PyMT+ model compared to Neu+ model as the levels of MuSC transcription factor Pax7 and MuSC differentiation regulator MyoD were significantly lower in skeletal muscle of PyMT+ mice compared to control mice [16]. We had previously reported loss of MyoD in the skeletal muscle of another Neu+ model, which carried an activated version of Neu and tumor latency in that model is shorter (~170 days) than the Neu+ model used in this study [34]. Thus, it appears that tumor growth rate has an influence on extent of molecular changes in skeletal muscle and can explain for differences in observations between acute xenograft cachexia models and chronic transgenic models. In this respect, a recent study reported beneficial effects of Il-15 supplementation in overcoming mammary

tumor-induced muscle fatigue in a syngeneic mouse model [60]. However, in both of our models, which cause relatively chronic muscle damage compared to acute muscle fatigue in their model (24 days), we did not observe any changes in Il-15 levels in tumor-bearing mice. In fact, in Neu+ model, improved muscle function upon DMAPT treatment correlated with lower Il-15. These results further emphasize the need to characterize cancer-induced skeletal muscle defect at individual or cancer subtype-specific levels instead of generalizing the findings from a model system.

Conclusions:

In a recent review, Baracos et al., [42] stated that "Our understanding of the underlying mechanisms of cachexia in individual patients is crude at best; accordingly, further characterization of the clinical etiologies is needed". Data presented here further support the concept that molecular features of skeletal muscle need to be evaluated at individual patient level or at least at tumor subtype level, similar to current attempts to characterize primary tumors at individual level or to subclassify tumors based on shared features. For example, we observed mitochondrial defects in PyMT+ model, whereas aging-associated defects were noted in Neu+ mice. Thus, characterizing skeletal muscle at individual or cancer subtype-specific levels will lead to better symptom management in future.

Supplementary Material

Refer to Web version on PubMed Central for supplementary material.

Acknowledgements:

We thank immunohistochemistry core, Multiplex Analysis Core and flow cytometry cores at the Indiana University Melvin and Bren Simon Cancer Center for providing supports. Department of Veterans Affairs merit award BX002764 funded this study (to HN).

List of Abbreviations:

Acvr2b	activin A receptor type 2B
ANOVA	analyses of variance
Carm1	co-activator associated arginine methyltransferase 1
Casz1	castor zinc finger 1
Ccl11	C-C motif chemokine ligand 11
CM	conditioned media
CO2	carbon dioxide
CoxIV	cytochrome c oxidase subunit 4 isoform 1
Cxcl1	C-X-C motif chemokine ligand 1
DMAPT	dimethylaminoparthenolide

DMEM	Dulbecco's modified eagles media
DOB	Date-of-Birth
ECM	extracellular matrix
EDL	extensor digitorum longus muscle
FBS	fetal bovine serum
G-csf	granulocyte-colony stimulating factor
Gm	Csf, granulocyte-macrophage colony stimulating factor
GTex	genotype-tissue expression
H&E	hematoxylin and eosin
Hey1	Hairy/enhancer-of-split related with YRPW motif protein 1
Hoxa9	homeobox A9
Ifnγ	interferon gamma
IHC	immunohistochemistry
IKK	Inhibitor of kappaB kinase
Il-1	interleukin 1
Il1ra	interleukin 1 receptor antagonist
Kmt2	Histone-lysine N-methyltransferase 2A
Mcp1	monocyte chemoattractant protein 1
Mdm2	Mouse double minute homolog 2
miRNA	microRNA
MMTV	mouse mammary tumor virus
Mip2	macrophage inflammatory protein 2
MuSC	muscle stem cells
Myf6	myogenic factor 6
MyoD	myoblast determination protein 1
NF-κB	nuclear factor-kappaB
Nurr1	Nuclear receptor related 1 protein
PCR	polymerase chain reaction
Pax7	paired box 7

Pgc1β	peroxisome proliferator-activated receptor gamma co-activator 1 (beta)
PyMT	polyoma middle tumor antigen
RIPA	radioimmunoprecipitation assay buffer
shRNA	short hairpin RNA
Smad7	mothers against decapentaplegic homolog 7
Tak1	transforming growth factor beta activated kinase
Tgfβ	transforming growth factor beta
Timp1	TIMP metallopeptidase inhibitor 1
Tnf	tumor necrosis factor

References:

1. Ness KK, Gurney JG, Zeltzer LK, Leisenring W, Mulrooney DA, Nathan PC, Robison LL, Mertens AC. The impact of limitations in physical, executive, and emotional function on health-related quality of life among adult survivors of childhood cancer: a report from the Childhood Cancer Survivor Study. Arch Phys Med Rehabil 2008, 89:128–136. [PubMed: 18164342]
2. Sweeney C, Schmitz KH, Lazovich D, Virnig BA, Wallace RB, Folsom AR. Functional limitations in elderly female cancer survivors. J Natl Cancer Inst 2006, 98:521–529. [PubMed: 16622121]
3. Kroenke CH, Rosner B, Chen WY, Kawachi I, Colditz GA, Holmes MD. Functional impact of breast cancer by age at diagnosis. J Clin Oncol 2004, 22:1849–1856. [PubMed: 15143077]
4. Michael YL, Kawachi I, Berkman LF, Holmes MD, Colditz GA. The persistent impact of breast carcinoma on functional health status: prospective evidence from the Nurses' Health Study. Cancer 2000, 89:2176–2186. [PubMed: 11147587]
5. Braithwaite D, Satariano WA, Sternfeld B, Hiatt RA, Ganz PA, Kerlikowske K, Moore DH, Slattery ML, Tammemagi M, Castillo A, et al. Long-term prognostic role of functional limitations among women with breast cancer. J Natl Cancer Inst 2010, 102:1468–1477. [PubMed: 20861456]
6. Song EJ, Lee CW, Jung SY, Kim BN, Lee KS, Lee S, Kang HS, Park IH, Lee MH, Kim YJ, et al. Prognostic impact of skeletal muscle volume derived from cross-sectional computed tomography images in breast cancer. Breast Cancer Res Treat 2018, 172:425–436. [PubMed: 30132218]
7. Waks AG, Winer EP. Breast Cancer Treatment: A Review. JAMA 2019, 321:288–300. [PubMed: 30667505]
8. Anderson WF, Rosenberg PS, Prat A, Perou CM, Sherman ME. How many etiological subtypes of breast cancer: two, three, four, or more? J Natl Cancer Inst 2014, 106.
9. Pfefferle AD, Herschkowitz JI, Usary J, Harrell JC, Spike BT, Adams JR, Torres-Arzayus MI, Brown M, Egan SE, Wahl GM, et al. Transcriptomic classification of genetically engineered mouse models of breast cancer identifies human subtype counterparts. Genome Biol 2013, 14:R125. [PubMed: 24220145]
10. Muller WJ, Sinn E, Pattengale PK, Wallace R, Leder P. Single-step induction of mammary adenocarcinoma in transgenic mice bearing the activated c-neu oncogene. Cell 1988, 54:105–115. [PubMed: 2898299]
11. de Matos-Neto EM, Lima JD, de Pereira WO, Figueredo RG, Riccardi DM, Radloff K, das Neves RX, Camargo RG, Maximiano LF, Tokeshi F, et al. Systemic Inflammation in Cachexia - Is Tumor Cytokine Expression Profile the Culprit? Front Immunol 2015, 6:629. [PubMed: 26732354]

12. Miyamoto Y, Hanna DL, Zhang W, Baba H, Lenz HJ. Molecular Pathways: Cachexia Signaling-A Targeted Approach to Cancer Treatment. Clin Cancer Res 2016, 22:3999–4004. [PubMed: 27340276]
13. Wang R, Nakshatri H. Systemic Actions of Breast Cancer Facilitate Functional Limitations. Cancers (Basel) 2020, 12.
14. Perkins ND. The diverse and complex roles of NF-kappaB subunits in cancer. Nat Rev Cancer 2012, 12:121–132. [PubMed: 22257950]
15. Calvani R, Marini F, Cesari M, Buford TW, Manini TM, Pahor M, Leeuwenburgh C, Bernabei R, Landi F, Marzetti E. Systemic inflammation, body composition, and physical performance in old community-dwellers. J Cachexia Sarcopenia Muscle 2017, 8:69–77. [PubMed: 27897412]
16. Wang R, Bhat-Nakshatri P, Padua MB, Prasad MS, Anjanappa M, Jacobson M, Finnearty C, Sefcsik V, McElyea K, Redmond R, et al. Pharmacological dual inhibition of tumor and tumor-induced functional limitations in transgenic model of breast cancer. Mol Cancer Ther 2017:2747–2758. [PubMed: 28978719]
17. Freudlsperger C, Bian Y, Contag Wise S, Burnett J, Coupar J, Yang X, Chen Z, Van Waes C. TGF-beta and NF-kappaB signal pathway cross-talk is mediated through TAK1 and SMAD7 in a subset of head and neck cancers. Oncogene 2013, 32:1549–1559. [PubMed: 22641218]
18. Nakshatri H, Bhat-Nakshatri P, Martin DA, Goulet RJ Jr., Sledge GW Jr. Constitutive activation of NF-kappaB during progression of breast cancer to hormone-independent growth. Mol Cell Biol 1997, 17:3629–3639. [PubMed: 9199297]
19. Guttridge DC, Mayo MW, Madrid LV, Wang CY, Baldwin AS Jr. NF-kappaB-induced loss of MyoD messenger RNA: possible role in muscle decay and cachexia [see comments]. Science 2000, 289:2363–2366. [PubMed: 11009425]
20. Cai D, Frantz JD, Tawa NE Jr., Melendez PA, Oh BC, Lidov HG, Hasselgren PO, Frontera WR, Lee J, Glass DJ, et al. IKKbeta/NF-kappaB activation causes severe muscle wasting in mice. Cell 2004, 119:285–298. [PubMed: 15479644]
21. Horak M, Novak J, Bienertova-Vasku J. Muscle-specific microRNAs in skeletal muscle development. Dev Biol 2016, 410:1–13. [PubMed: 26708096]
22. Liu L, Charville GW, Cheung TH, Yoo B, Santos PJ, Schroeder M, Rando TA. Impaired Notch Signaling Leads to a Decrease in p53 Activity and Mitotic Catastrophe in Aged Muscle Stem Cells. Cell Stem Cell 2018, 23:544–556 e544. [PubMed: 30244867]
23. Schworer S, Becker F, Feller C, Baig AH, Kober U, Henze H, Kraus JM, Xin B, Lechel A, Lipka DB, et al. Epigenetic stress responses induce muscle stem-cell ageing by Hoxa9 developmental signals. Nature 2016, 540:428–432. [PubMed: 27919074]
24. Alexander MS, Rozkalne A, Colletta A, Spinazzola JM, Johnson S, Rahimov F, Meng H, Lawlor MW, Estrella E, Kunkel LM, et al. CD82 Is a Marker for Prospective Isolation of Human Muscle Satellite Cells and Is Linked to Muscular Dystrophies. Cell Stem Cell 2016, 19:800–807. [PubMed: 27641304]
25. Magli A, Incitti T, Kiley J, Swanson SA, Darabi R, Rinaldi F, Selvaraj S, Yamamoto A, Tolar J, Yuan C, et al. PAX7 Targets, CD54, Integrin alpha9beta1, and SDC2, Allow Isolation of Human ESC/iPSC-Derived Myogenic Progenitors. Cell Rep 2017, 19:2867–2877. [PubMed: 28658631]
26. Kumar B, Prasad MS, Bhat-Nakshatri P, Anjanappa M, Kalra M, Marino N, Storniolo AMV, Rao X, Liu S, Wan J, et al. Normal breast-derived epithelial cells with luminal and intrinsic subtype-enriched gene expression document inter-individual differences in their differentiation cascade. Cancer Res 2018, 78:5107–5123. [PubMed: 29997232]
27. Sander H, Wallace S, Plouse R, Tiwari S, Gomes AV. Ponceau S waste: Ponceau S staining for total protein normalization. Anal Biochem 2019, 575:44–53. [PubMed: 30914243]
28. Brooks HL, Lindsey ML. Guidelines for authors and reviewers on antibody use in physiology studies. Am J Physiol Heart Circ Physiol 2018, 314:H724–H732. [PubMed: 29351459]
29. Fosang AJ, Colbran RJ. Transparency Is the Key to Quality. J Biol Chem 2015, 290:29692–29694. [PubMed: 26657753]
30. Feige P, Brun CE, Ritso M, Rudnicki MA. Orienting Muscle Stem Cells for Regeneration in Homeostasis, Aging, and Disease. Cell Stem Cell 2018, 23:653–664. [PubMed: 30388423]

31. Torres-Palsa MJ, Koziol MV, Goh Q, Cicinelli PA, Peterson JM, Pizza FX. Expression of intercellular adhesion molecule-1 by myofibers in mdx mice. Muscle Nerve 2015, 52:795–802. [PubMed: 25728314]
32. Gundry RL, Raginski K, Tarasova Y, Tchernyshyov I, Bausch-Fluck D, Elliott ST, Boheler KR, Van Eyk JE, Wollscheid B. The mouse C2C12 myoblast cell surface N-linked glycoproteome: identification, glycosite occupancy, and membrane orientation. Mol Cell Proteomics 2009, 8:2555–2569. [PubMed: 19656770]
33. Gurova KV, Hill JE, Guo C, Prokvolit A, Burdelya LG, Samoylova E, Khodyakova AV, Ganapathi R, Ganapathi M, Tararova ND, et al. Small molecules that reactivate p53 in renal cell carcinoma reveal a NF-kappaB-dependent mechanism of p53 suppression in tumors. Proc Natl Acad Sci U S A 2005, 102:17448–17453. [PubMed: 16287968]
34. Chen D, Goswami CP, Burnett RM, Anjanappa M, Bhat-Nakshatri P, Muller W, Nakshatri H. Cancer Affects microRNA Expression, Release, and Function in Cardiac and Skeletal Muscle. Cancer Res 2014, 74:4270–4281. [PubMed: 24980554]
35. Thomas JK, Mir H, Kapur N, Bae S, Singh S. CC chemokines are differentially expressed in Breast Cancer and are associated with disparity in overall survival. Sci Rep 2019, 9:4014. [PubMed: 30850664]
36. Villeda SA, Luo J, Mosher KI, Zou B, Britschgi M, Bieri G, Stan TM, Fainberg N, Ding Z, Eggel A, et al. The ageing systemic milieu negatively regulates neurogenesis and cognitive function. Nature 2011, 477:90–94. [PubMed: 21886162]
37. Karin M, Greten FR. NF-kappaB: linking inflammation and immunity to cancer development and progression. Nat Rev Immunol 2005, 5:749–759. [PubMed: 16175180]
38. Guzzoni V, Ribeiro MBT, Lopes GN, de Cassia Marqueti R, de Andrade RV, Selistre-de-Araujo HS, Durigan JLQ. Effect of Resistance Training on Extracellular Matrix Adaptations in Skeletal Muscle of Older Rats. Front Physiol 2018, 9:374. [PubMed: 29695977]
39. Rheinlander A, Schraven B, Bommhardt U. CD45 in human physiology and clinical medicine. Immunol Lett 2018, 196:22–32. [PubMed: 29366662]
40. Guy CT, Cardiff RD, Muller WJ. Induction of mammary tumors by expression of polyomavirus middle T oncogene: a transgenic mouse model for metastatic disease. Mol Cell Biol 1992, 12:954–961. [PubMed: 1312220]
41. Guy CT, Webster MA, Schaller M, Parsons TJ, Cardiff RD, Muller WJ. Expression of the neu protooncogene in the mammary epithelium of transgenic mice induces metastatic disease. Proc Natl Acad Sci U S A 1992, 89:10578–10582. [PubMed: 1359541]
42. Baracos VE, Martin L, Korc M, Guttridge DC, Fearon KCH. Cancer-associated cachexia. Nat Rev Dis Primers 2018, 4:17105. [PubMed: 29345251]
43. Wada E, Tanihata J, Iwamura A, Takeda S, Hayashi YK, Matsuda R. Treatment with the anti-IL-6 receptor antibody attenuates muscular dystrophy via promoting skeletal muscle regeneration in dystrophin-/utrophin-deficient mice. Skelet Muscle 2017, 7:23. [PubMed: 29078808]
44. Dumitru A, Radu BM, Radu M, Cretoiu SM. Muscle Changes During Atrophy. Adv Exp Med Biol 2018, 1088:73–92. [PubMed: 30390248]
45. Lukjanenko L, Karaz S, Stuelsatz P, Gurriaran-Rodriguez U, Michaud J, Dammone G, Sizzano F, Mashinchian O, Ancel S, Migliavacca E, et al. Aging Disrupts Muscle Stem Cell Function by Impairing Matricellular WISP1 Secretion from Fibro-Adipogenic Progenitors. Cell Stem Cell 2019, 24:433–446 e437. [PubMed: 30686765]
46. Margolis LM, Lessard SJ, Ezzyat Y, Fielding RA, Rivas DA. Circulating MicroRNA Are Predictive of Aging and Acute Adaptive Response to Resistance Exercise in Men. J Gerontol A Biol Sci Med Sci 2017, 72:1319–1326. [PubMed: 27927764]
47. Buckingham M, Rigby PW. Gene Regulatory Networks and Transcriptional Mechanisms that Control Myogenesis. Dev Cell 2014, 28:225–238. [PubMed: 24525185]
48. Mitchell CJ, D'Souza RF, Schierding W, Zeng N, Ramzan F, O'Sullivan JM, Poppitt SD, Cameron-Smith D. Identification of human skeletal muscle miRNA related to strength by high-throughput sequencing. Physiol Genomics 2018, 50:416–424. [PubMed: 29602299]

49. Boscolo Sesillo F, Fox D, Sacco A. Muscle Stem Cells Give Rise to Rhabdomyosarcomas in a Severe Mouse Model of Duchenne Muscular Dystrophy. Cell Rep 2019, 26:689–701 e686. [PubMed: 30650360]
50. Zhang Z, Cherryholmes G, Mao A, Marek C, Longmate J, Kalos M, Amand RP, Shively JE. High plasma levels of MCP-1 and eotaxin provide evidence for an immunological basis of fibromyalgia. Exp Biol Med (Maywood) 2008, 233:1171–1180. [PubMed: 18535166]
51. Akkaya N, Atalay NS, Selcuk ST, Alkan H, Catalbas N, Sahin F. Frequency of fibromyalgia syndrome in breast cancer patients. Int J Clin Oncol 2013, 18:285–292. [PubMed: 22322540]
52. Srikuea R, Symons TB, Long DE, Lee JD, Shang Y, Chomentowski PJ, Yu G, Crofford LJ, Peterson CA. Association of fibromyalgia with altered skeletal muscle characteristics which may contribute to postexertional fatigue in postmenopausal women. Arthritis Rheum 2013, 65:519–528. [PubMed: 23124535]
53. Pierson E, Consortium GT, Koller D, Battle A, Mostafavi S, Ardlie KG, Getz G, Wright FA, Kellis M, Volpi S, et al. Sharing and Specificity of Co-expression Networks across 35 Human Tissues. PLoS Comput Biol 2015, 11:e1004220. [PubMed: 25970446]
54. Kim E, Lembert M, Fallata GM, Rowe JC, Martin TL, Satoskar AR, Reo NV, Paliy O, Cormet-Boyaka E, Boyaka PN. Intestinal Epithelial Cells Regulate Gut Eotaxin Responses and Severity of Allergy. Front Immunol 2018, 9:1692. [PubMed: 30123215]
55. He WA, Berardi E, Cardillo VM, Acharyya S, Aulino P, Thomas-Ahner J, Wang J, Bloomston M, Muscarella P, Nau P, et al. NF-kappaB-mediated Pax7 dysregulation in the muscle microenvironment promotes cancer cachexia. J Clin Invest 2013, 123:4821–4835. [PubMed: 24084740]
56. Borzi C, Calzolari L, Centonze G, Milione M, Sozzi G, Fortunato O. mir-660-p53-mir-486 Network: A New Key Regulatory Pathway in Lung Tumorigenesis. Int J Mol Sci 2017, 18.
57. Hunten S, Kaller M, Drepper F, Oeljeklaus S, Bonfert T, Erhard F, Dueck A, Eichner N, Friedel CC, Meister G, et al. p53-Regulated Networks of Protein, mRNA, miRNA, and lncRNA Expression Revealed by Integrated Pulsed Stable Isotope Labeling With Amino Acids in Cell Culture (pSILAC) and Next Generation Sequencing (NGS) Analyses. Mol Cell Proteomics 2015, 14:2609–2629. [PubMed: 26183718]
58. Behera AK, Bhattacharya A, Vasudevan M, Kundu TK. p53 mediated regulation of coactivator associated arginine methyltransferase 1 (CARM1) expression is critical for suppression of adipogenesis. FEBS J 2018, 285:1730–1744. [PubMed: 29575726]
59. Molchadsky A, Ezra O, Amendola PG, Krantz D, Kogan-Sakin I, Buganim Y, Rivlin N, Goldfinger N, Folgiero V, Falcioni R, et al. p53 is required for brown adipogenic differentiation and has a protective role against diet-induced obesity. Cell Death Differ 2013, 20:774–783. [PubMed: 23412343]
60. Bohlen J, McLaughlin SL, Hazard-Jenkins H, Infante AM, Montgomery C, Davis M, Pistilli EE. Dysregulation of metabolic-associated pathways in muscle of breast cancer patients: preclinical evaluation of interleukin-15 targeting fatigue. J Cachexia Sarcopenia Muscle 2018, 9:701–71v4. [PubMed: 29582584]

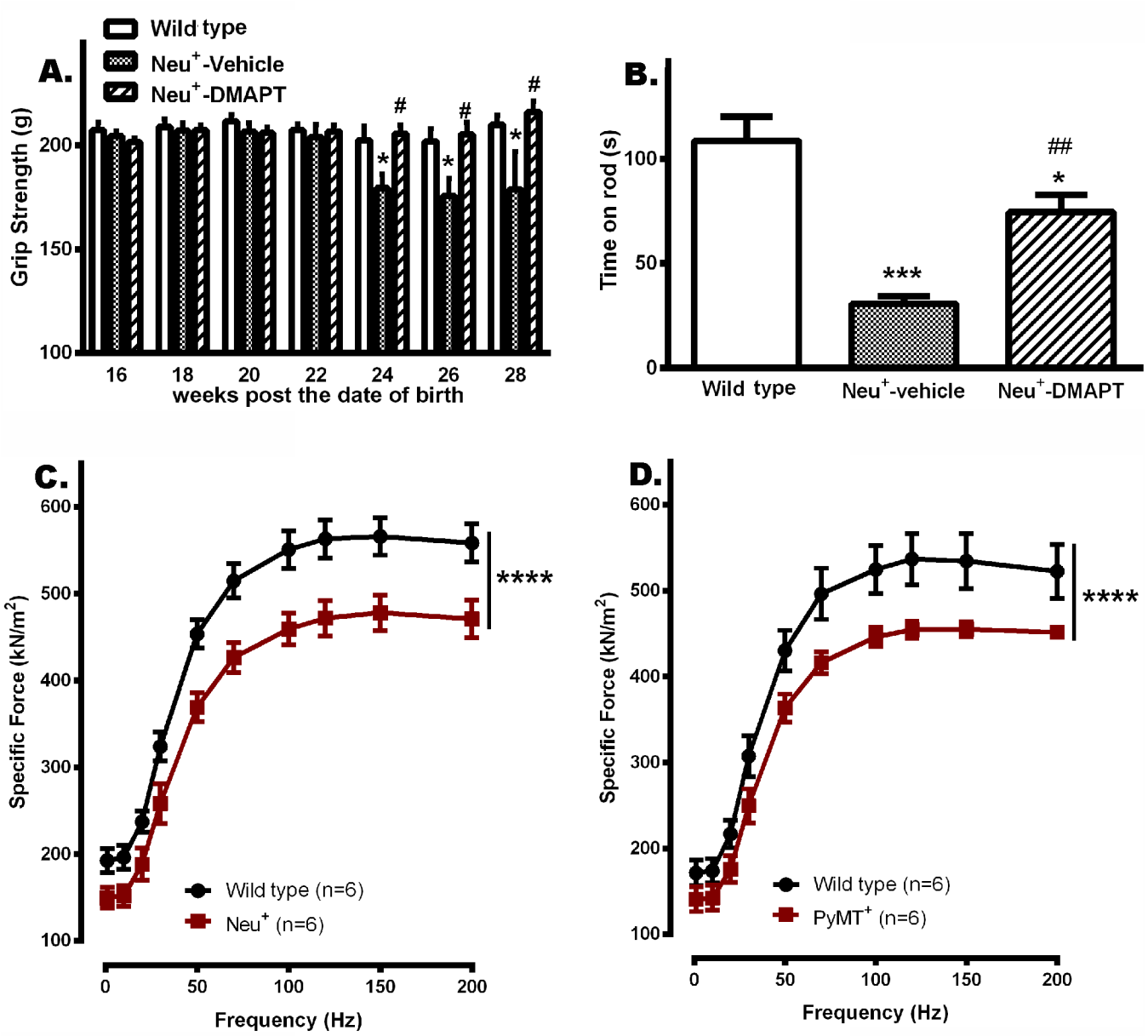

Figure 1:

Functional limitations in mammary tumor-bearing mice. **A.** Reduced grip strength force in mammary tumor-bearing Neu+ mice was restored upon oral administration of DMAPT (n=8–12; p=0.0069). **B.** Reduced rotarod performance in mammary tumor-bearing Neu+ mice was reversed by DMAPT treatment (n=8–12, p<0.0001). * indicates significance between wild type and tumor-bearing groups. # indicates significance between vehicle-treated tumor-bearing group and DMAPT-treated tumor-bearing group. **C.** Skeletal muscle of tumor-bearing Neu+ mice displayed lower contraction force compared to age and sex-matched controls (p<0.0001). **D.** Tumors in PyMT+ mice similarly affected skeletal muscle contraction force (p<0.0001).

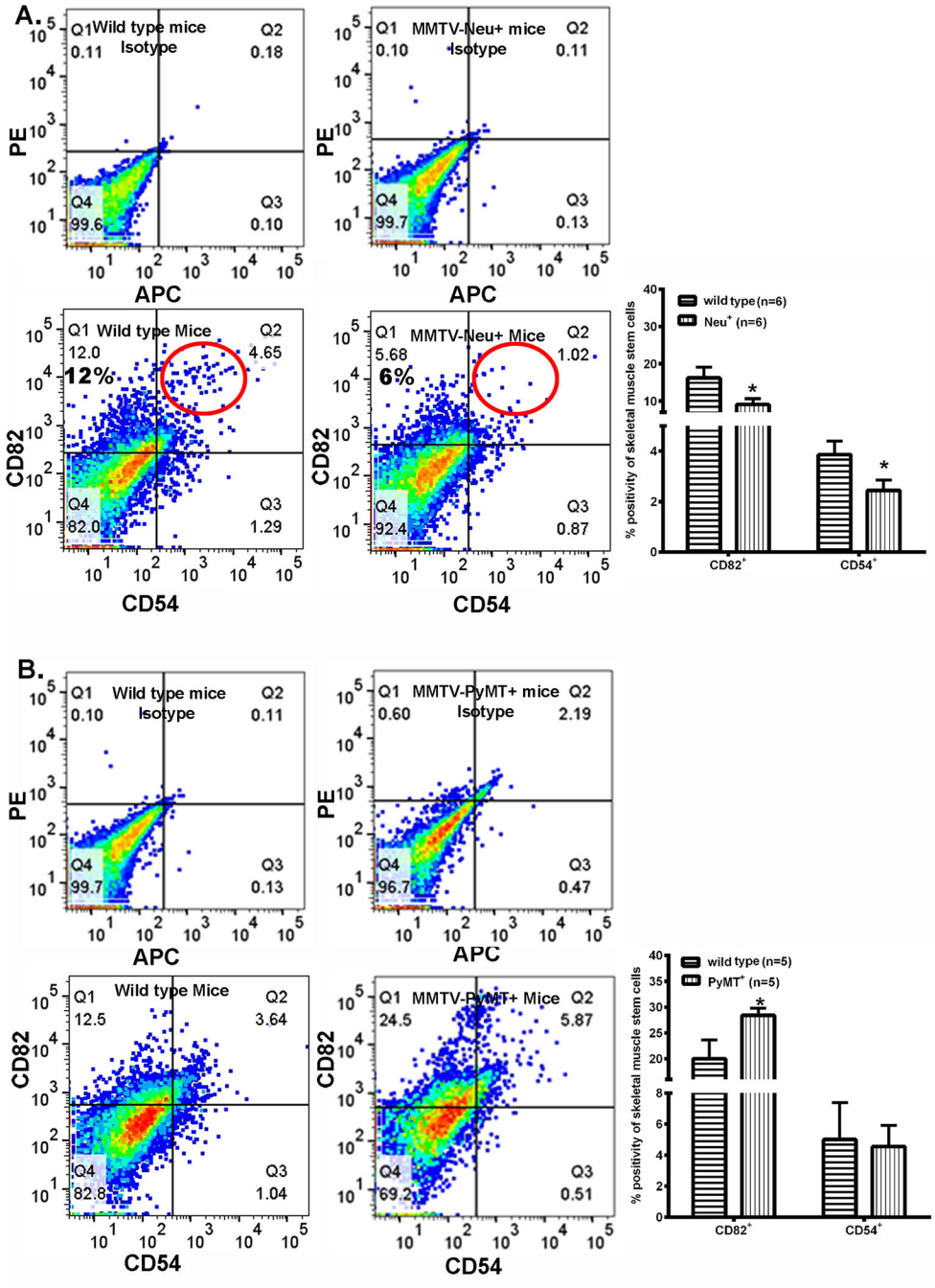

Figure 2:

Altered levels of CD82+ and CD54+ stem/progenitor cells in the skeletal muscle of tumor-bearing mice. **A.** Skeletal muscle of Neu+ mice contained lower number of CD82+ (p=0.0407) and CD54+ cells (top panel, p=0.0431). Circles denote CD82+/CD54+ double positive cells. **B.** Skeletal muscle composition in PyMT+ mice is different from that of Neu+ mice as there were higher numbers of CD82+ cells (p=0.0416) without any changes in CD54+ cells (bottom panel).

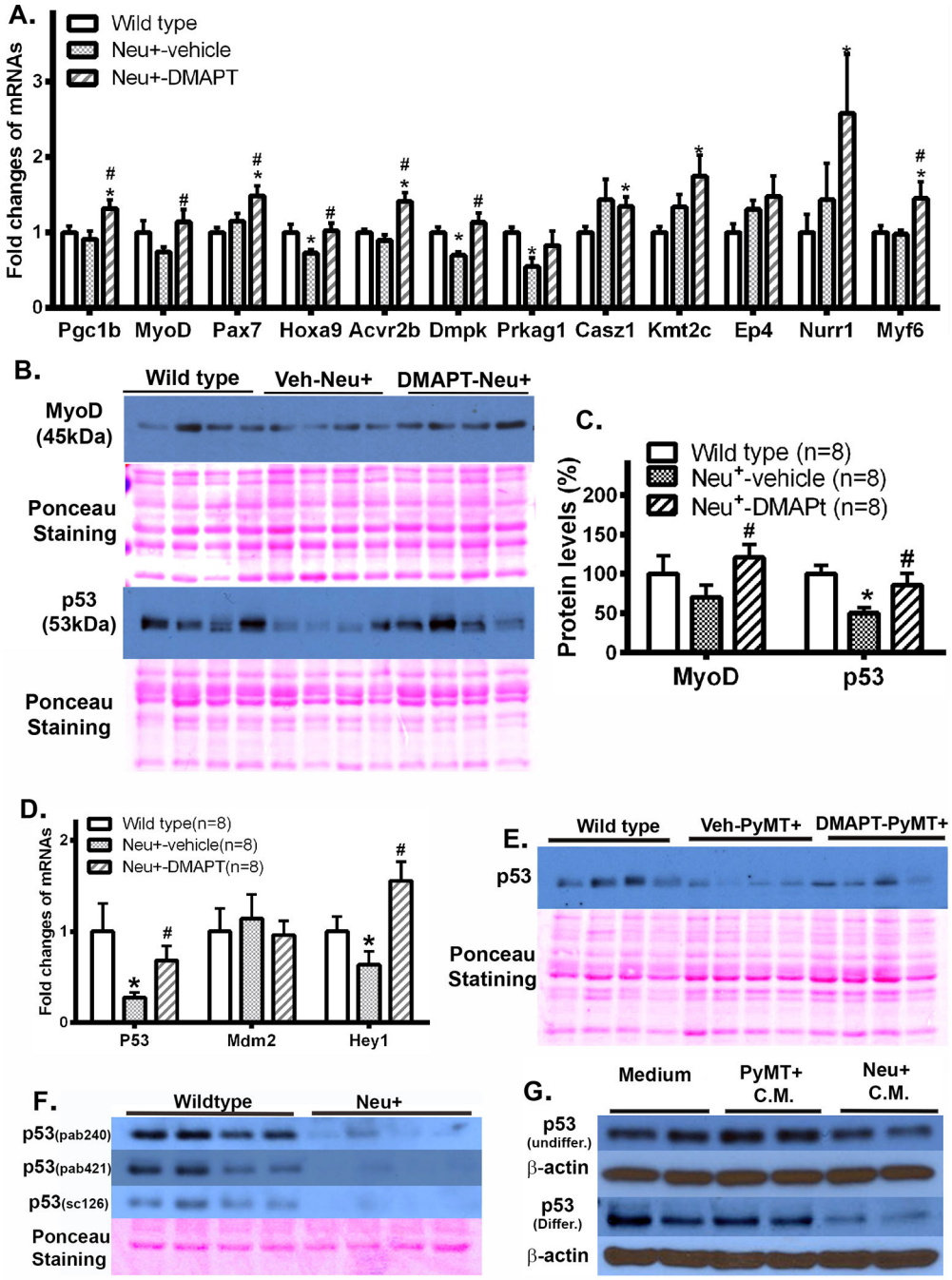

Figure 3:

The effect of Neu+ tumor on gene expression in the skeletal muscle. **A.** Expression pattern of skeletal muscle-enriched genes in wild type, Neu+, and Neu+ DMAPT-treated mice (n=8–12). **B.** MyoD and p53 protein levels in the skeletal muscle of indicated mice (four per group). Same blots were stained with Ponceau Staining to demonstrate equal loading. **C.** Quantitative analyses of western blots using the Image J software (p=0.0452). **D.** mRNA levels of p53 (p=0.0311), Mdm2 and Hey1 (0.0472) in the skeletal muscle of Neu+ mice. * indicates significance between wild type group and tumor-bearing groups. # indicates

significance between vehicle-treated tumor-bearing group and DMAPT-treated tumor-bearing group. **E.** p53 protein levels were lower in the skeletal muscle of PyMT+ mice, which could be reversed by DMAPT treatment ($p=0.0092$). **F.** Depletion of p53 protein in the purified skeletal muscle cells of Neu+ mice ($p<0.0001$). **G.** Conditioned medium (CM) from Neu+ ($p=0.0409$), but not PyMT+, tumor-derived cell line downregulated p53 in differentiated but not undifferentiated C2C12 myoblast cell line.

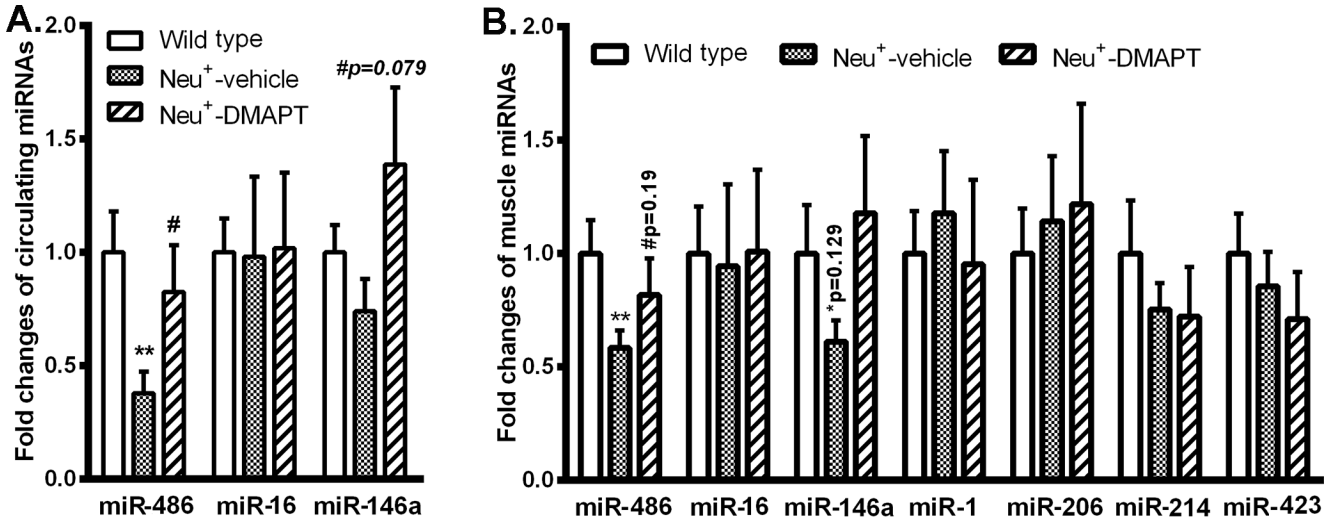

Figure 4:

Tumor-induced changes in miRNAs in circulation and in skeletal muscles. **A.** Circulating miR-486 was lower in Neu+ mice, which was reversed by DMAPT treatment (n=8–12, p=0.0049). **B.** Skeletal muscle miR-486 was lower in Neu+ mice (p=0.022), which was partially reversed by DMAPT treatment (n=8–12). * indicates significance between wild type group and tumor-bearing groups. # indicates significance between vehicle-treated tumor-bearing group and DMAPT-treated tumor-bearing group.

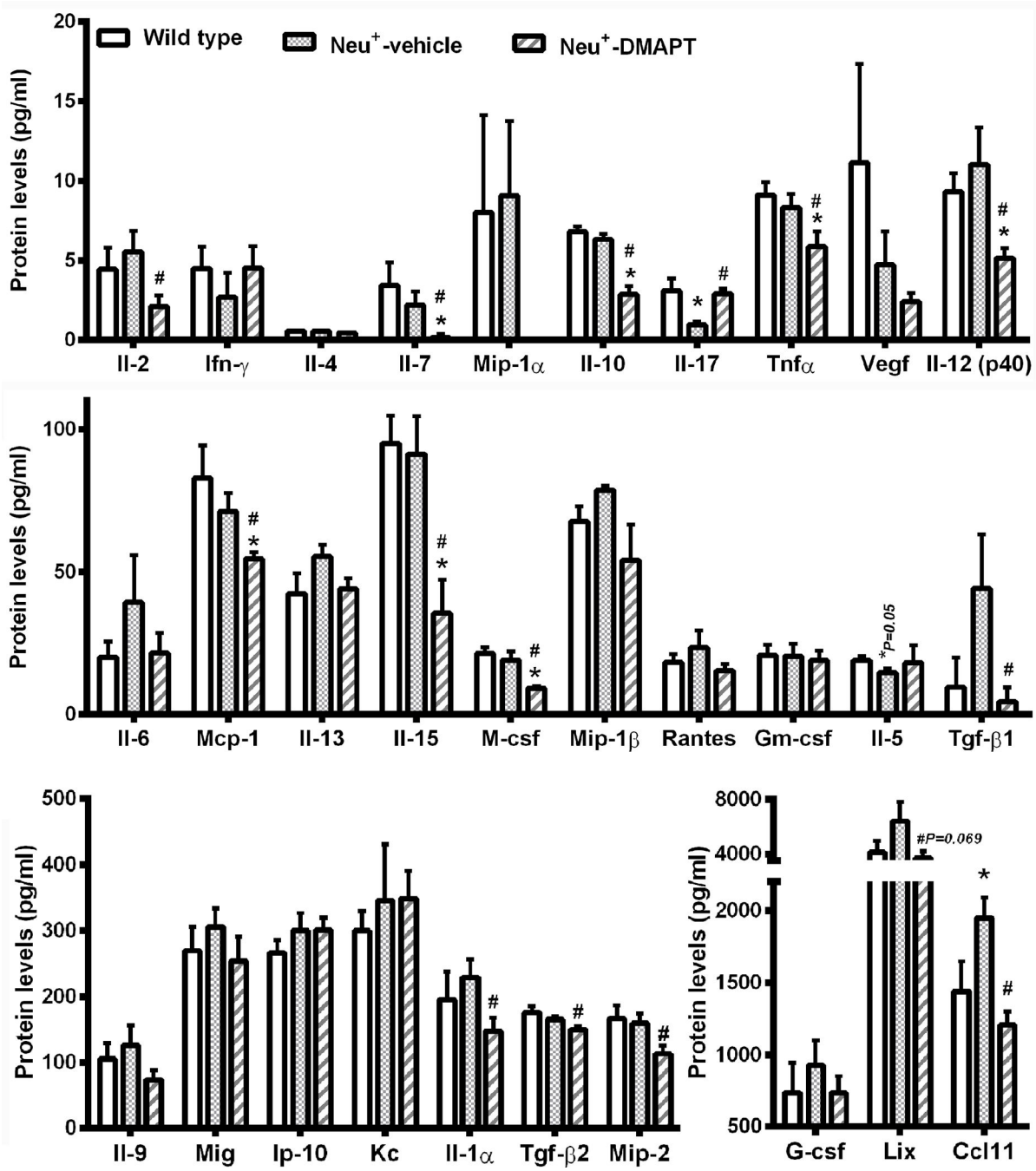

Figure 5:

Circulating cytokines/chemokines in Neu+ mice. Cytokine/chemokine levels in plasma of age-matched animals of three groups were assessed using multiplex ELISA kit (n=6 per group). In case of no detectable cytokine/chemokine, a value of zero was given. Only data with at least three animals per group with detectable expression were included. Data were graphed in four panels based on cytokine/chemokine levels. * indicates significance between wild type group and tumor-bearing group ($p<0.05$). # indicates significance between vehicle-treated tumor-bearing group and DMAPT-treated tumor-bearing group ($p<0.05$).

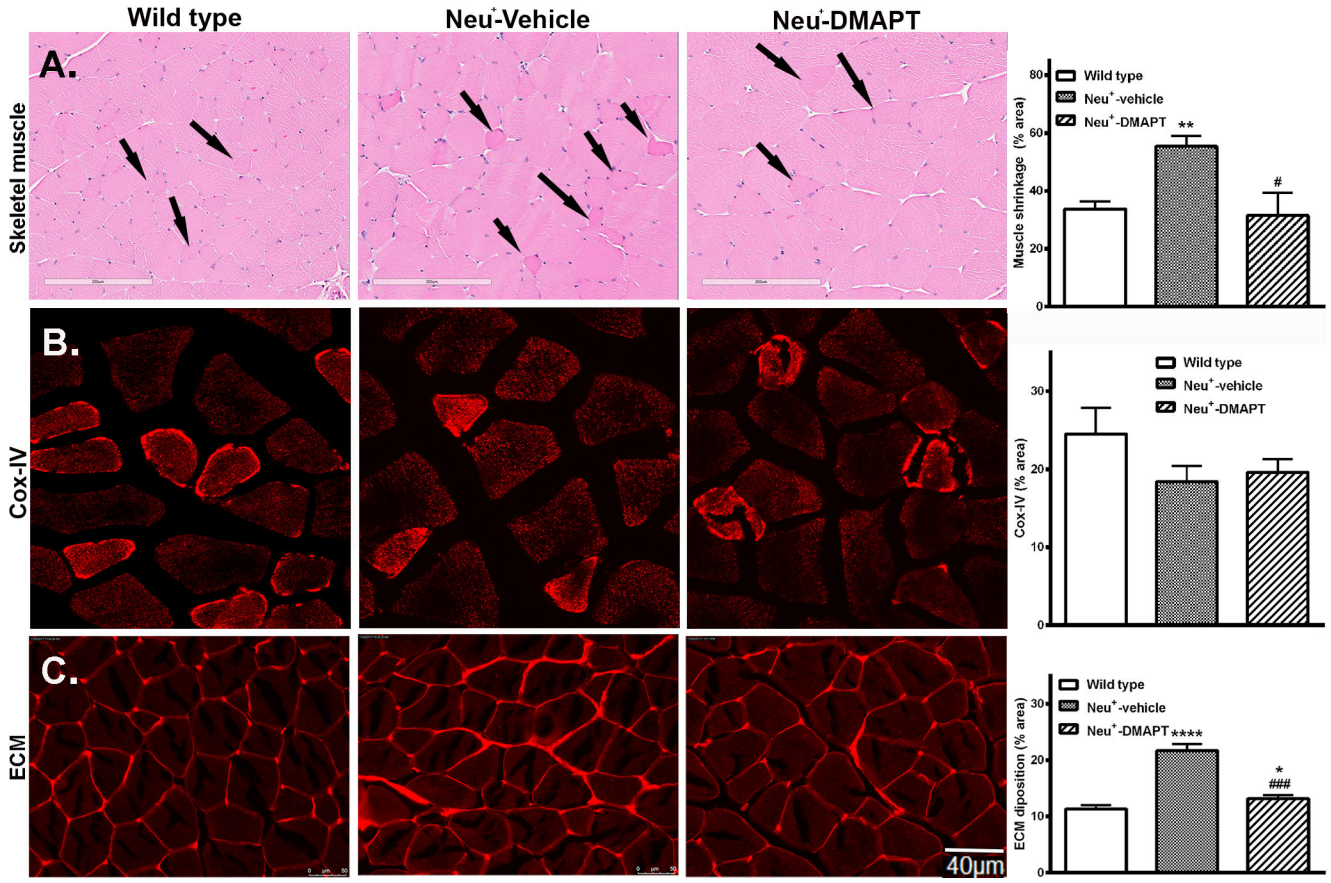

Figure 6:

Morphological changes in the skeletal muscles of Neu+ mice. **A**. Mammary tumors led to significant shrinkage of muscle fibers in Neu+ mice compared to wild type mice. DMAPT treatment reversed muscle shrinkage (top row). Arrows indicate shrunk muscle cells (n=6, p=0.0033). **B.** Mitochondria content in muscles was measured through IHC of Cox IV. No significant changes between groups (n=8; middle row). **C.** ECM in the skeletal muscles of Neu+ tumor-bearing mice was higher compared to wild type mice, which was reversed by DMAPT treatment (n=8; bottom row, p<0.0001). * indicates significance between wild type group and tumor-bearing groups. # indicates significance between vehicle-treated tumor-bearing group and DMAPT-treated tumor-bearing group.

Table 1.

Molecular changes in transgenic mouse models of breast cancer

Categories	Molecules	PyMT+ mice		Neu+ mice	
Drug	**DMAPT**	**−**	**+**	**−**	**+**
Muscle mRNAs	Pax7	low	restored	No effect	Up
	MyoD	low	low	low trend	Restored
	Pgc1β	low	restored	No effect	Up
	Acvr2b	low	restored	No effect	Up
	Dmpk	low	restored	Low	Restored
	Lmna	Low trend	low		
	Prkag1	low	low	Low	up trend
	Hoxa9	low	restored	Low	Restored
	Casz1			No effect	Up
	Kmt2c			No effect	Up
	Nurr1			No effect	Up
	Myf6			No effect	Up
	p53	low	restored	Low	Restored
	Mdm2	No effect	No effect	No effect	No effect
	Hey1	low trend	No effect	low	Restored
Muscle proteins	Pax7	low	restored		
	MyoD	low trend	restored	low trend	Restored
	p53	low	restored	Low	Restored
	Cox-IV	low	restored	No effect	No effect
Cell surface markers	CD45			Up	Up
	CD82	up		Low	
	CD54	No effect		Low	
Muscle miRNAs	miR-486	low	low	Low	up trend
	miR-16	low	low	No effect	No effect
	miR-146a	low	low	low trend	up trend
	miR-214	low	low	No effect	No effect
	miR-206	low	low	N/A	N/A
Circulating miRNAs	miR-486	low	up trend	Low	Restored
	miR-146a	No change	up	No effect	No effect
Circulating cytokines	Il-5	No change	low	Low	up trend
	Tnfα	up	up	No effect	Low
	Mip-2	low	restored	No effect	Low
	Il-9	low	restored	No effect	No effect
	Kc	low	low	No effect	No effect
	Il-1a	low	restored	No effect	Low
	G-csf	up	up	No effect	No effect

Categories	Molecules	PyMT$^+$ mice		Neu$^+$ mice	
Drug	**DMAPT**	−	+	−	+
	Tgf-β1	N/A	N/A	up trend	Restored
	Tgf-β2	up	up	No effect	Low
	Tgf-β3	up trend	up	Not detected	Not detected
	Lix	low	restored	up trend	Restored
	Eotaxin (Ccl11)	No effect	No effect	up	Restored